Electrokinetics of nitrite to ammonia conversion in the neutral medium over a platinum surface

Md. Fahamidul Islam [a, b], Hassan Shahriar Ifti [a], Mostafizur Rahman [c], Kentaro Aoki [d], Yuki Nagao [d], Ali Aldalbahi [c], Jamal Uddin [e], Mohammad A. Hasnat [a, *]

[a] *Electrochemistry & Catalysis Research Laboratory (ECRL), Department of Chemistry, School of Physical Sciences, Shahjalal University of Science and Technology, Sylhet-3114, Bangladesh*

[b] *Department of Chemistry, Faculty of Science, Noakhali Science and Technology University, Noakhali-3814, Bangladesh*

[c] *Department of Chemistry, College of Science, King Saud University, P.O. Box 2455, Riyadh 11451, Saudi Arabia*

[d] *School of Materials Science, Japan Advanced Institute of Science and Technology, 1-1 Asahidai, Nomi, Ishikawa, 923-1292, Japan*

[e] *Department of Natural Sciences, Coppin State University (CSU), Baltimore, MD, USA*

**Corresponding author:*

Mohammad A. Hasnat, E-mail: mah–che@sust.edu,

Abstract

Polycrystalline Pt electrode was employed to selectively convert nitrite ions (NO_2^-) into useful nitrogenous compound through electrochemical reduction reaction in neutral medium. According to adsorptive stripping analysis, the reduction process produced nitric oxide (NO) on the surface of Pt electrode. The spectroscopic test and gas chromatographic studies discovered the presence of ammonia (NH_3) in the electrolyzed solution, suggesting the transformation of adsorbed NO into NH_3 during the reverse scan. Scan rate dependent investigation was performed to elucidate kinetic information relating to this reaction on Pt surface. From E_p vs scan rate (υ) and j_p vs υ (logarithmic plot), it was found that the conversion of NO_2^- ion into NO is an irreversible reaction which relies

on the diffusion of NO_2^- ions to electrode surface. The Tafel analysis unveiled that the first electron transfer sets the overall reaction rate, having formal reduction potential, $E^{0'} = -0.46$ V and standard heterogeneous rate constant, $k^0 = 1.07 \times 10^{-2}$ cm s^{-1}. Reductive transfer coefficient (α) is another kinetics parameter, which was found to be approximate 0.77 from the difference between E_p and $E_{p/2}$ of the voltammograms obtained over scan rate range 0.005 V s^{-1} to 0.250 V s^{-1}, indicating a stepwise process. According to temperature-dependent voltammograms, the nitrite reduction reaction on Pt had a calculated activation energy of about 19.8 kJ mol^{-1} and a pre-exponential factor of about 8.39×10^3 mA cm^{-2}.

Key words: Nitrite, nitric oxide, ammonia, platinum electrode, kinetics, activation energy

1. Introduction

Nitrite ion (NO_2^-) is regarded as a toxic nitrogenous species which is ubiquitous in ecosystem and is evolved as a stable intermediate from other nitrogenous species used in agriculture, aquaculture, chemical industries, and pharmaceutical industries [1–3]. Due to excessive use of nitrogenous compounds in agriculture and aquaculture, the aquatic lives, mainly fish, are exposing to high level of nitrites which adversely affects fish growth, blood oxygen carrying capacity, molting, osmoregulation, water balance and causing endocrine disruption [3].

Humans are also directly exposing to nitrite ions by consuming meat and fish that are preserved with nitrite salts [2]. Drinking of nitrates/nitrites contaminated groundwater is another reason behind nitrite accumulation in human body [2]. The primary physiological impact of nitrite ions on people is its role in the conversion of regular Hb to metHb, which cannot carry oxygen to cells [4–8]. Due to nitrite ion exposure, lack of oxygen supply in tissues becomes evident when the concentration of metHb hits 10 % of the regular Hb concentration and this condition is known as methemoglobinemia in clinical terminology. As a result of this blood condition, the color of body tissues begin to appear blue, which is called cyanosis and acute nitrite exposure often leads to breathing difficulties, called asphyxia [4–8]. Humans typically have metHb levels of less than 2%, and babies younger than 3 months typically have levels of less than 3%.[4–8]. It has been established that nitrite and nitrosatable substances in the human stomach can combine to create N-

nitroso compounds. Even though some of the most readily formed N-nitroso compounds, like N-nitrosoproline, are not carcinogenic in people, many of these N-nitroso compounds have been found to be carcinogenic in all the animal species examined [4–9]. The N-nitroso chemicals that cause cancer in some animal species also most likely cause cancer in human [4–8].

Besides being a potential carcinogenic substance, nitrite ion is an indirect driver of global warming since nitrous oxide (N_2O) is generated as main product from nitrite ion in biological denitrification and microbial nitrification processes [3,10]. N_2O is regarded as one of the most dangerous greenhouse gases after methane (CH_4) and carbon dioxide (CO_2). Even some reports claim that the gas has 310 times more global warming potential than carbon dioxide over 100-years' time span [3].

In order to address these environmental and health issues, the presence of nitrite ions in water has raised concerns among scientists, prompting them to research effective methods for their removal from water. Conventional physicochemical techniques, such as ion exchange, reverse osmosis, and electrodialysis, enable efficient removal of nitrate/nitrite ions but typically fall short of their total disposal. On the other hand, the majority of environmentally friendly techniques rely on microorganisms that selectively convert nitrate/nitrite to nitrogen [9,11–13]. The biological process is lengthy, intricate, and frequently necessitates expensive post-treatment of effluents. However, electrochemical or electrocatalytic treatment is fast and product selective because of specific electrode and potential selection. Consequently, it is possible to covert nitrite ions into useful nitrogenous compounds like NH_4^+ or, NH_3, N_2, NO_2, HNO_2, NH_2OH, by performing electrochemical reduction reaction [14–17]. Conversion of nitrate/nitrite to nitrogen is a mostly desired root in the context of wastewater treatment since nitrogen is a harmless species [18]. Other than water purification, the generation of ammonia/ammonium ion from nitrite/nitrate is also appreciated in various aspects [19–21]. For instance, ammonia is an important component for producing ammonium nitrate (NH_4NO_3), which is widely used as fertilizer [20]. In the textile industry, ammonia is used to soften cotton and to fabricate synthetic fiber [20]. In recent times, ammonia has been highly appreciated as a clean energy source because it can provide hydrogen without emitting any carbon [21]. Note that ammonia in its liquid state has greater volumetric hydrogen than liquid hydrogen, and it is easily storable as well [21,22]. In the field of energy production, ammonia is indirectly utilized in developing a battery called an aqueous ammonium ion battery, as the ammonium ion, conjugate acid of ammonia, is able to move rapidly in an

aqueous medium under the influence of a potential gradient [19]. It is worth noting that the rapid movement of the ammonium ion is due to its light weight and small hydrodynamic radius [19]. Moreover, ammonia is also utilized for organic syntheses, refrigeration, and antimicrobial drug production [20].

Over the years, various electro-catalysts have been evolved to investigate the reduction of nitrite ions and frequently used electro-catalysts are generally based on transition metals such as, titanium (Ti) [23–25], nickel (Ni) [26], copper (Cu) [27], ruthenium (Ru) [28], rhodium (Rh) [17,29,30], palladium (Pd) [31–34], silver (Ag) [35], platinum (Pt) [36–42]. Pt has garnered the most attention among these catalysts for use in the nitrate/nitrite reduction reaction because of its ability to transform nitrite ions selectively into products that are not toxic and have added value. For instance, M. Duca *et al*., [37] looked into the mechanism behind the nitrate reduction reaction that took place on a polycrystalline Pt electrode at varying pH levels. They found that adsorbed nitric oxide (NO) acted as an intermediate species in acidic and slightly acidic medium, converting into N_2O and NH_2OH as the reaction progressed. In contrast, the sole product produced was NH_4^+ ion through the generation of NH_2OH as an intermediary in basic medium. In a separate study, M Duca *et al*., [39] demonstrated the reduction of NO_2^- ion to N_2 on Pt electrode having 110 facets in 0.1 M NaOH solution. Based on voltametric and online electrochemical mass spectrometry, they proposed a tentative mechanism for N_2 formation. In brief, the initial step of NO_2^- ion reduction results in the formation of adsorbed NH_2 species, which subsequently undergoes further reduction reaction with NO_2^- ion present in the solution phase, ultimately yielding N_2. In order to gain insight into the denitrification of nitrates/nitrite, Chun *et al*., [41] conducted an investigation on electro-reduction of NO, a crucial intermediate in the denitrification process, on the surface of a Pt 100 electrode in acidic medium. The conversion of NO to $NH_4^+$was observed through the formation of adsorbed NOH species, as determined by density functional theory (DFT) and kinetic Monte Carlo (kMC) analyses.

The preceding discourse indicates that scholars have conducted thorough investigations into the mechanistic pathway of NO_2^- electro-reduction on Pt electrode in both acidic and basic media. To date, no scholarly research has been conducted that provides a comprehensive explanation of the conversion of NO_2^- ions into a specific product under neutral conditions, accompanied by a thorough analysis of the kinetics involved. Therefore, in this work, we endeavored to perform the electrochemical reduction of NO_2^- ions on Pt electrode in neutral medium. Herein, we took

advantage of voltammetry, UV-visible spectroscopic method, and gas chromatography to identify the resultant product generated during the process of NO_2^- ion electrochemical reduction. Moreover, the voltametric technique was utilized to elucidate the proper kinetic and thermodynamic information regarding the electrochemical reduction of NO_2^- ions in neutral condition.

2. Experimental

2.1. Chemicals

To conduct this experiment, analytical grade chemicals *e.g.*, sodium nitrite ($NaNO_2$), Potassium Chloride (KCl), Hydroxylamine (NH_2OH), Sulphuric acid (H_2SO_4) and Alumina slurry (Al_2O_3) were purchased from Germany's renowned Sigma Aldrich and Merck. These chemicals were used without further refining. Milli-Q water (resistivity >18.2 MΩ cm^{-1}) was used to prepare all the required solutions for this experiment.

2.2. Instrumentation

In order to carry out electrochemical experiments, three different electrochemical Potentiostats *e.g.*, CHI 660E (CHI Instruments, USA), Autolab PGSTAT20 and Wavedirive20 (PINEIncorp. USA), were utilized. For the purpose of carrying out the electrochemical investigations, a one-compartment electrochemical cell that was outfitted with a conventional three-electrode system was used. A Teflon covered polycrystalline Pt electrode with a diameter of 3 mm was used as the working electrode for each measurement. Pt wire was used as the auxiliary electrode, and Ag/AgCl (sat. KCl) was used as the reference electrode.

2.3. Electrode pretreatment

A series of treatments were performed to achieve a Pt electrode surface that is free of contamination. The pre-treatment process was involved the utilisation of alumina slurry (0.03 μm) to polish the surface of Pt electrode for a duration of 10 minutes. Subsequently, the electrode underwent a thorough rinsing process with deionized water, followed by a 10-minute sonication treatment in deionized water. Finally, the electrode was voltammetrically pretreated via continuous cycling within the potential range of − 0.2-1.5 V in a 0.1 M H_2SO_4 solution at a scan rate of 0.1 V s^{-1} for a duration of 30 minutes.

2.4. Electrochemical experiment

All of the experiments except temperature effect on nitrite reduction reaction were performed at 25 °C. As supporting electrolyte, solution of KCl salt was used for all of the investigations. For voltametric experiments, the cleaned Pt electrode was first scanned in 2.0 M KCl solution by applying 0 to −1.0 V against A/AgCl (sat. KCl) reference electrode. Then the electrode was scanned in 2.0 M KCl containing 1.0 M $NaNO_2$ solution in the similar potential range. Note that the scan rate was 0.005 V s^{-1} in both cases. For XPS experiment, the linear sweep voltametric data were taken by applying potential of −0.4 V to −0.95 V against Ag/AgCl (sat. KCl) reference electrode to a Pt wire in 2.0 M KCl + 1.0 M $NaNO_2$ solution at scan rate of 0.005 V s^{-1}.

For scan rate dependent experiment, the linear sweep voltammograms were obtained by scanning the Pt electrode in 2.0 M KCl solution having 1.0 M $NaNO_2$ by gradually increasing the scan rates from 0.005 to 0.250 V s^{-1}.

In the case of both spectroscopic and chromatographic experiments, the voltametric experiments were performed in a similar fashion. Concisely, a volume of 10 mL of 2.0 M KCl containing 1.0 M $NaNO_2$ solution was placed in an electrochemical cell to perform the voltametric experiment. Following that, the solution was electrolyzed using a three-electrode setup, with Pt serving as the working electrode, Ag/AgCl (sat. KCl) as reference electrode, Pt wire as counter electrode and the Pt electrode was scanned for 200 cycles in the potential range of 0 to −0.95 V at 0.005 V s^{-1}scan rate.

During the temperature dependent investigation, in which temperatures ranged from 20 °C to 60 °C, the electrochemical set-up was submersed in a small water tank and voltametric experiments were carried out once the desired temperature was reached and maintained within the cell. The temperature was validated by measuring the temperature of the solution within the electrochemical cell.

2.5. X-ray photoelectron spectroscopic investigation

The presence of N 1*s* and O 1*s* of NH_2OH was investigated by using X-ray photoelectron spectroscopy (XPS). Just after the linear sweep voltammetry, Pt electrode was thoroughly washed with deionized water, dried in air and immediately measured. Delay-line detector (DLD) spectrometer (Kratos Axis-Ultra; Kratos Analytical Ltd.) with an Al *K*α radiation source (1486.6 eV) was used eject electron from the target species. The conductive carbon tape was used to attach the sample, and each spectrum was calibrated against C 1*s* peak at 284.8 eV as the inner reference.

Obtained spectra were fitted using XPSPEAK 4.1 software with the subtraction of the background by Shirley method.

2.6. Absorptive stripping experiment

Initially, a clean Pt electrode was used in a freshly solution of 2.0 M KCl containing 1.0 M $NaNO_2$ for multiple linear sweep voltametric studies in the range of −0.5 V to −0.95 Vat scan rate of 0.005 V s^{-1}. After that the electrode surface was rinsed with deionized water to ensure the NO_2^- ion free surface and transferred to another electrochemical cell where only 2.0 M KCl solution was present. Subsequently, the Pt electrode was subjected to potential scanning in the range −0.5 V to −0.95 V at scan rate of 0.005 V s^{-1}.

2.7. Spectroscopic investigation

To detect the presence of NH_3 in solution, the investigation involved the utilization of a Milwaukee MI 405 ammonia medium range meter. Briefly, the electrolyzed solution was taken into a cuvette, which was thereafter inserted into the holder of the ammonia meter. Subsequently, the meter was initialized by pressing the zero button on the meter, following the usual operational method provided with the instrument. Afterwards, the cuvette was detached from the holder and 4 droplets of reagent-1 (provided by Milwaukee) and 4 droplets of reagent-2 (also provided by Milwaukee) were sequentially introduced into the solution. Once the reagent was added correctly, the cuvette was gently swirled to achieve a uniform mixture. The cuvette was again positioned in the holder, and the measurement was promptly recorded. It is important to mention that the same procedure was followed to confirm the existence of NH_3 in the sodium nitrite solution.

2.8. GC-Mass investigation

The Gas Chromatography-Mass Spectrometry (GC-MS) instrument utilized to identify the solution phase species in electrochemical reduction of nitrite ion on a Pt electrode was the GCMS-QP2020 type manufactured by Shimadzu Corporation, Japan. The solution electrolyzed solution was used for GC-MS experiment. During the identification process, the oven and injection temperature were 35 and 270 ºC, respectively. The detection process was performed in split mode with a split ratio of 90:1.

3. Results and discussion

3.1. Reduction of NO_2^- ion on Pt electrode

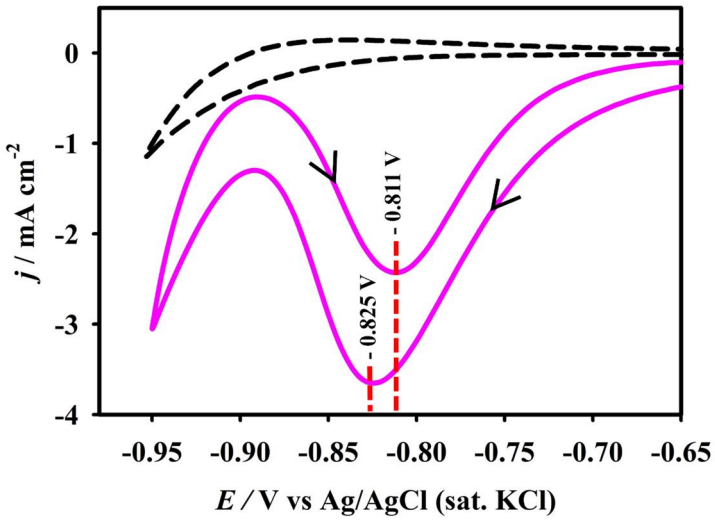

Figure 1. Cyclic voltammograms of polycrystalline Pt electrode in 2.0 M KCl and 1.0 M $NaNO_2$ at scan rate of 0.005 V s^{-1}.

Figure 1 portrays the cyclic voltammogram of Pt electrode recorded in 2.0 M KCl solution containing 1.0 M $NaNO_2$ at scan rate of 0.005 V s^{-1}. An intense reduction wave is seen to appear at around –0.822 V vs Ag/AgCl (std. KCl) during forward scan, indicating the reduction of nitrite ions on Pt electrode surface, whereas another intense reduction wave is appeared at ca. –0.806 V in reverse scan. Primarily, it could be assumed that the reverse wave appeared due to reduction of adsorbed species on Pt surface formed in forward scan. According to previous literature, most probable adsorbed species are nitric oxide (NO), hydroxylamine (NH_2OH) or, ammonium ion (NH_4^+) under acidic pH [37,38,41]. In this regard, we took advantage of XPS to confirm the formation of adsorbed species on Pt surface by taking XPS spectra of Pt before and after performing nitrite reduction reaction via LSV method. At first, the XPS of a freshly Pt surface was taken and no nitrogenous species were found in the spectrum. Then the LSV experiments were performed for 50 times by utilizing the Pt surface in 2.0 M KCl solution containing 1.0 M $NaNO_2$ at 0.005 V s^{-1} scan rate. After that, the XPS experiments were performed and the obtained spectra revealed the presence of nitrogenous species on the Pt surface (**see Fig. S1 in supporting information**).

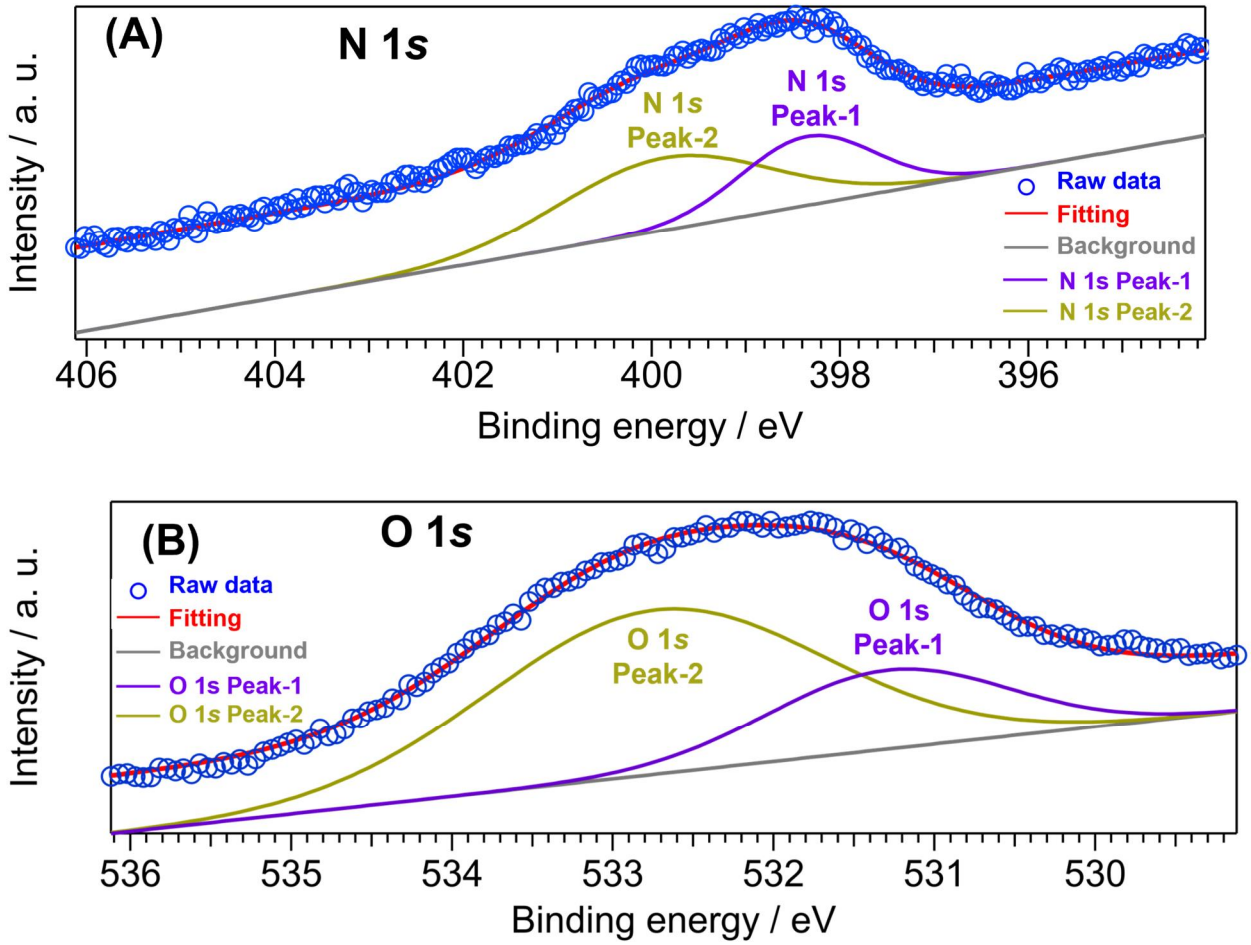

Figure 2. (A) and (B) Fitted XPS spectra of N 1*s* and O 1*s* Pt plate after performing reduction reaction.

From figure 2(A) and (B), it is seen that there are two N 1s peaks at 398.19 eV and 399.71 eV, respectively and two peaks for O 1s at 531.29 eV and 532.73 eV on Pt surface. The appearance of these peaks after voltametric experiment confirms the formation of adsorbed nitrogenous species on Pt surface in nitrite reduction reaction. The spectra, however, do not identify if the species is NO, NH_2OH or NH_4^+. It is worth mentioning that, within these group of species, the probability of NH_4^+ ion as an adsorbed species can be excluded due to its non-reducible nature. Therefore, the probable adsorbed species on Pt after voltametric experiment is either NO or NH_2OH.

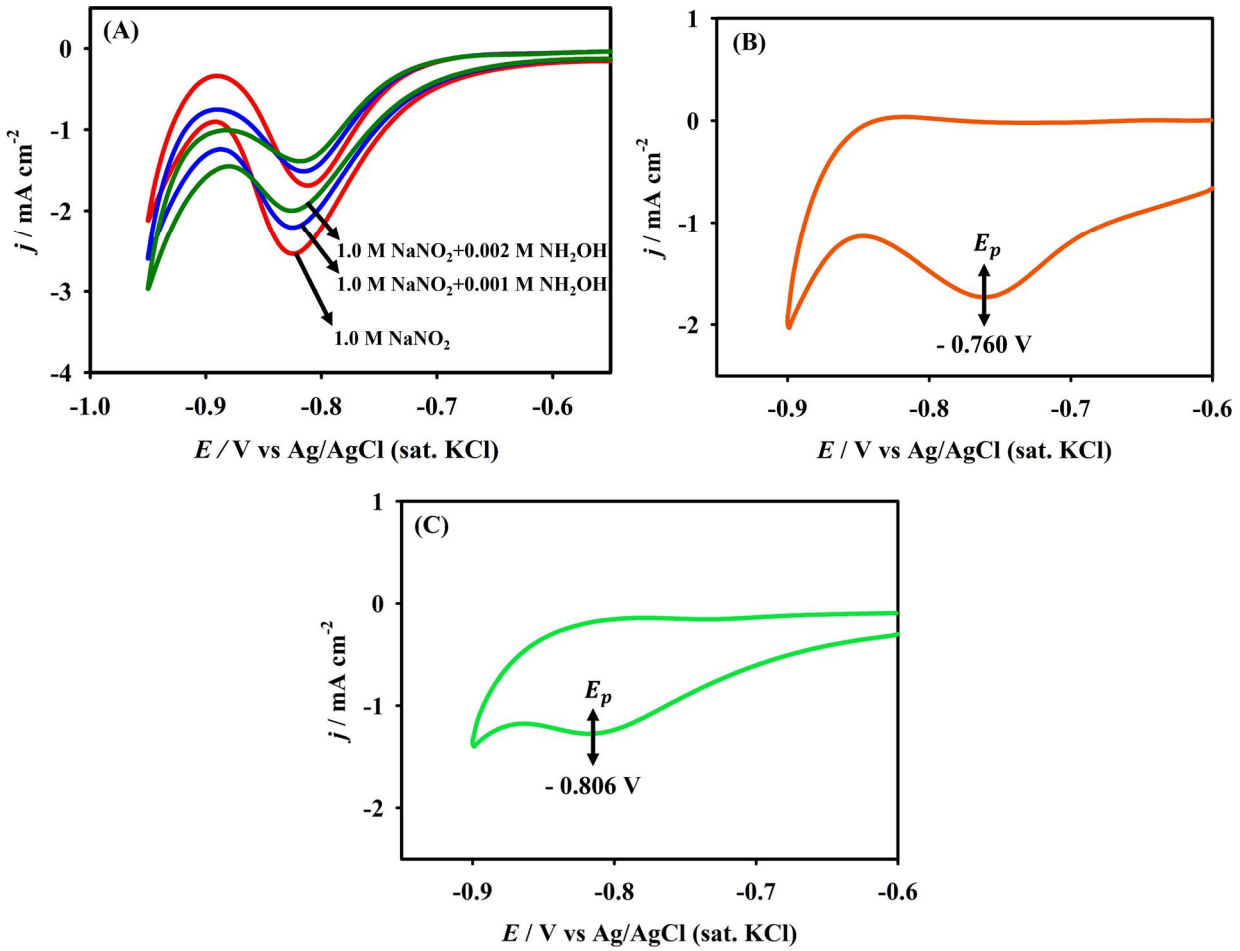

Figure 3. (A) Cyclic voltammograms of polycrystalline Pt electrode in 2.0 M KCl containing 1.0 M $NaNO_2$, 1.0 M $NaNO_2$ + 0.001 M NH2OH and 1.0 M $NaNO_2$ + 0.002 M NH_2OH; (B) Cyclic voltammogram of NH_2OH reduction in 2.0 M KCl solution on Pt electrode after adsorption of NH_2OH by soaking the electrode in 0.5 M NH_2OH solution for 5 minutes.; (C) Stripped cyclic voltammogram in 2.0 M KCl solution recorded by means of Pt electrode after performing several linear sweep voltametric experiments in another cell containing 2.0 M KCl and 1.0 M $NaNO_2$. In all cases the scan rate was 0.005 V s^{-1}.

Assuming that the species being NH_2OH, we investigated nitrite reduction reaction by adding NH_2OH dropwise in the electrochemical cell containing 2.0 M KCl and 1.0 M $NaNO_2$ solution. It was found that the height of the peak in the reverse scan decreases rather increasing. This observation rules out NH_2OH as the anticipated intermediate, formed in the forward scan during nitrite reduction reaction. To further validate this finding, a clean Pt electrode was immersed in freshly prepared 0.5 M NH_2OH solution for 5 minutes to form an adsorbed layer of NH_2OH on Pt.

Subsequently, the electrode was transferred to another electrochemical cell containing N_2 saturated 2.0 M KCl solution and CV was taken in the potential range of −0.6 V to −0.90 V at scan rate of 0.005 V s^{-1}, as shown in **Figure 3 (B)**.

Next, we performed adsorptive stripping experiment to check the resemblance between NH_2OH and adsorbed layer on Pt surface in nitrite reduction reaction. As shown in **Figure 3 (C)**, the peak potential of the obtained stripped CV is the same as that of the reverse scan in NO_2^- ion reduction (**Figure 1**).

It is obvious from the F**igure 3 (B) & (C)** that the NH_2OH reduction CV does not resemble stripped CV found due to reduction of adsorbed species formed during electrochemical reduction of NO_2^- ion. More specifically, the shape of stripped CV, onset potential, peak potential, charging current density as well as Faradic current density are completely different from the CV of adsorbed NH_2OH reduction. Thus, it can be inferred that the adsorbed species formed on Pt surface is, in fact, NO, as per equation (1). It is worth mentioning that the adsorbed species being NO in this context is also supported by transition metal nitrosyl coordination bond through some back-bonding hypothesis [43].

$$NO_2^- + 4H^+ + 1e^- \rightarrow NO + 2H_2O \qquad (1)$$

Next, to determine the species present in the solution phase, we employed the Nessler reagent after completing 200 cycles using a Pt electrode in a 2.0 M KCl solution in presence of 1.0 M $NaNO_2$. Upon the addition of Nessler reagent solution, a product of brown hue was observed in the Nessler test. And the reading on the spectrometer at 430 nm revealed that the electrolyzed solution contained approximately 1.50 parts per million (ppm) of NH_3. In order to validate the finding, the freshly produced electrolyzed solution was again studied using gas chromatography-mass spectrometry (GC-MS). The spectrum unambiguously demonstrated the existence of NH_3 ion within the electrolyzed solution (**see Fig. S2 in supporting information**). Thus, it may be inferred that the reverse scan shown in Fig. 1 occurred as a result of the conversion of adsorbed NO into NH_3 as the final product as per equation (2).

$$NO + 5H^+ + 5e^- \rightarrow NH_3 + H_2O \qquad (2)$$

3.2. Kinetics of NO_2^- ion Reduction on Pt electrode

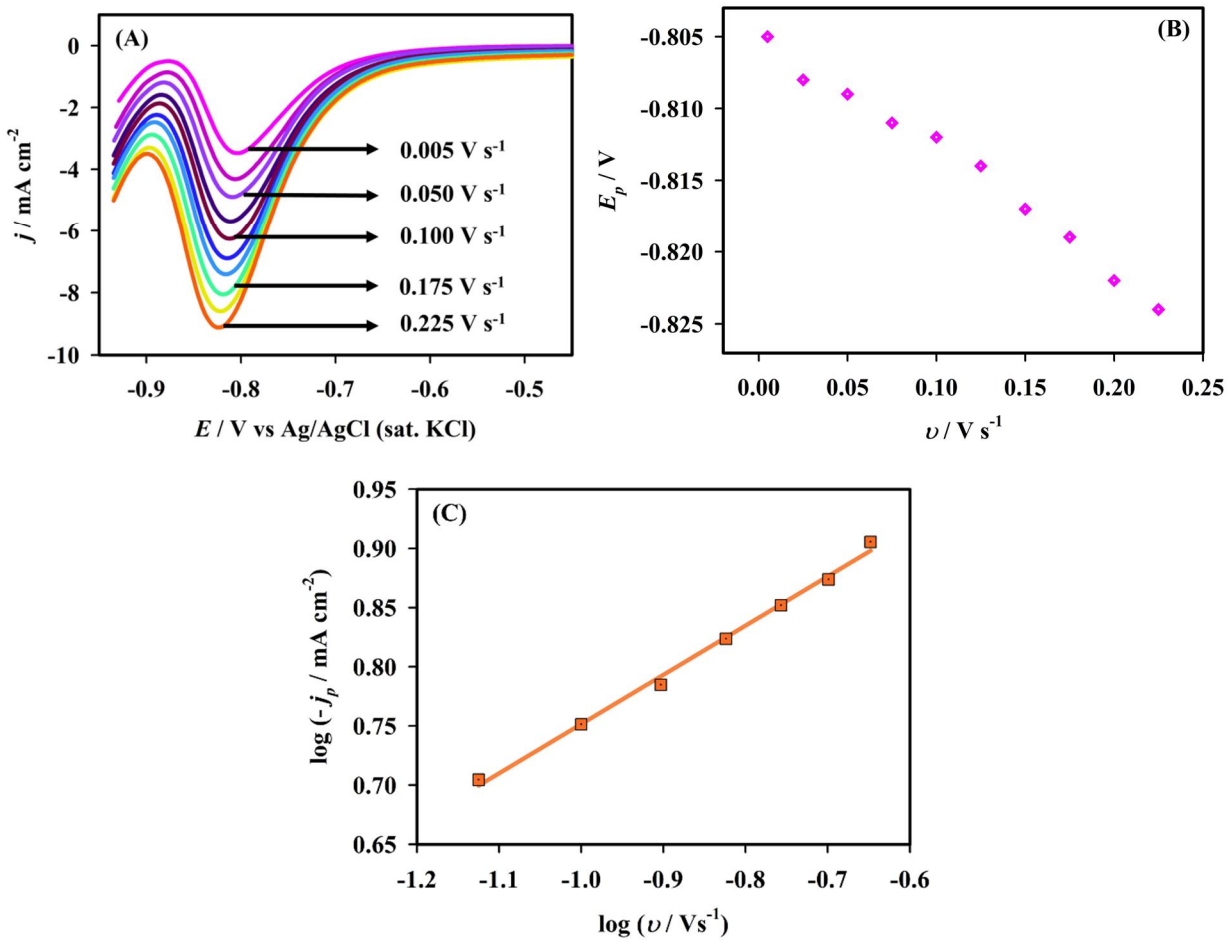

Figure 4. (A) Scan rate dependent cyclic voltammograms of 2.0 M KCl + 1.0 M $NaNO_2$ solution at Pt electrode obtained in the range of 0.005 V s^{-1} to 0.225 V s^{-1}. (B) Dependence of peak potential on scan rate at Pt electrode. (C) Relation between log ($-j_p$) and log (υ) of nitrite reduction reaction at Pt surface.

To unravel the kinetics of nitrite reduction reaction on Pt electrode, scan rate effect on the reaction was carefully studied since scan rate dependent voltammograms bears important kinetic and mechanistic information like, electron transfer coefficient, heterogeneous rate constant, formal potential for an electrochemical reaction. Therefore, linear sweep voltammograms of 1.0 M $NaNO_2$ in 2.0 M KCl were recorded by means of polycrystalline Pt electrode at varying scan rates (0.005 V s^{-1} to 0.225 V s^{-1}), as shown in **Fig. 4(A)**. From figures 4(A) & (B), it is obvious that the peak current density (j_p) increases with the increase in scan rate, while peak potential (E_p) shifts negatively. The observed features indicate that the nitrite reduction reaction on Pt surface is fully irreversible reaction [44]. The logarithmic form of Randle's-Sevick equation is frequently

employed to determine whether an electrode process is governed by diffusion or adsorption in the case of an irreversible electrode reaction [45,46]. Therefore, logarithmic current densities were plotted against logarithmic scan rates (**see Fig. 4(C)**), as per equation (3) [45,46]

$$log\, j_p = log\ \gamma + \frac{1}{2} log\, v \qquad (3)$$

Here, $\gamma = (2.99 \times 10^5) nC\alpha D^{\frac{1}{2}}$

Where, n = number of electron transfer, C = bulk concentration (mol cm^{-3}), D = diffusion coefficient (cm^2 s^{-1}), α = reductive transfer coefficient and v = scan rate (V s^{-1}). From regression analysis, the slope value of the logarithmic plot was found to be 0.49 (r^2 : 0.99), inferring that the nitrite reduction reaction on Pt electrode is diffusion-controlled electrode process [45,46].

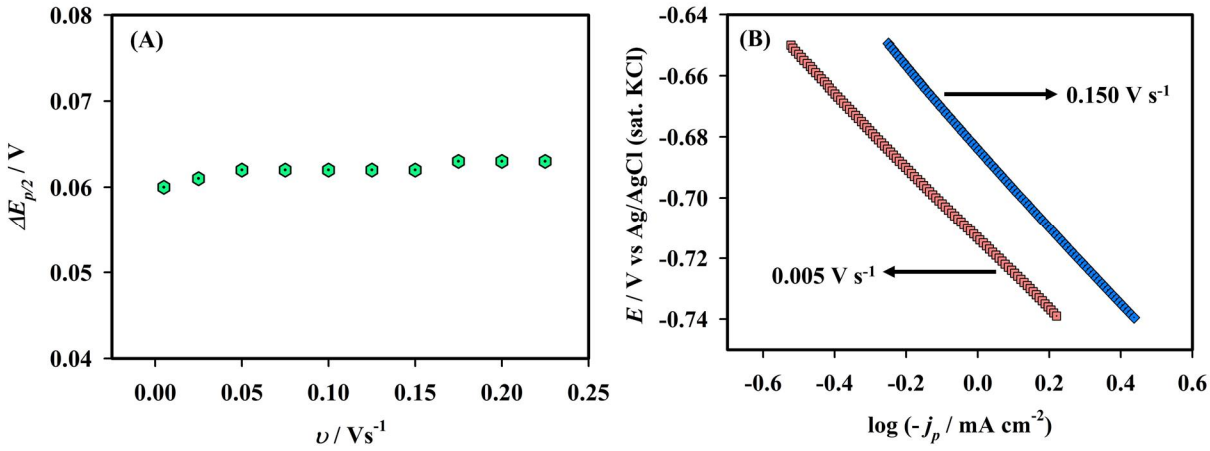

Figure 5. (A) Dependence of $\Delta E_{p/2}$ on scan rate (υ) for nitrite reduction reaction on Pt electrode. (B) Tafel plot. Data were derived from Fig. 4(A).

Next, the difference between peak potential (E_p) and half peak potential ($E_{p/2}$), that is, $\Delta E_{p/2}$ was calculated from scan rate dependent voltammograms to unfold the kinetics of the electrode process and was evaluated to be 61±1 mV in the range of 0.005 V s^{-1} to 0.225 V s^{-1}, as shown in **Fig. 5(A)**. As the value of $\Delta E_{p/2}$ remained almost unchanged over the scan rates, so the nitrite reduction reaction on Pt electrode followed Butler-Volmer Kinetic model [44,47,48]. Hence, Tafel slope was estimated within the kinetic limited region of voltammogram regarding nitrite reduction reaction. From scan rate dependent voltammograms, the Tafel slope (see **Fig. 5(B)**) was found to be 128 ± 10 mV dec^{-1} which signifies the involvement of an electron transfer in rate determining step [44]. In previous studies, it has been shown that reduction of nitrite ions takes place through the

formation of nitric oxide (NO) on Pt electrode surface in acidic and neutral media [37,38]. In present case, the value of Tafel slope also supports the formation NO which determines the overall reaction rate.

In relevance with **Fig. 4(A)**, the Tafel equation was fitted to calculate the formal reduction potential (E^0) of nitrite reduction reaction on Pt electrode since applied potential (E) is related to the logarithmic faradic current (log (j)) as per equation (4) [45,47].

$$E = (E^{0\prime} - b \times \log(j_0)) + b \times \log(j) \quad (4)$$

Where, $b = \frac{2.303RT}{\alpha F}$ is the Tafel slope and j_0 is exchange current density.

But, to evaluate $E^{0'}$ from intercept of Tafel plot, it is necessary to know the value of j_0, which in turn is related to standard heterogeneous rate constant (k^0) through the equation $j_0 = nFCk^0$. In case of irreversible electrode reaction, it is possible to determine the value of k^0 by using equation (5) [49]. It is indeed worth mentioning that the equation (5) is applicable to the reduction (or, oxidation) wave at the scan rate (υ), where mass transfer limited current does not change satisfactorily.

$$k^0 = \frac{1.11\sqrt{D}\sqrt{\vartheta}}{\sqrt{E_p - E_{p/2}}} \quad (5)$$

In this study, the linearity of j_p vs $\upsilon^{1/2}$ deviated at around 0.3 V s^{-1}, therefore, the value of k^0 was estimated to be 1.07×10^{-2} cm s^{-1} by evaluating the peak width at this scan rate. Finally, the value of formal potential for nitrite reduction reaction was calculated to be -0.46 V on Pt electrode. To unfold reaction mechanistic pathway, transfer coefficient (α) was then evaluated from $\Delta E_{p/2}$, as these parameters are related to each other by the equation (6) [44,48].

$$\alpha = \frac{1.857RT}{F\,|E_p - E_{\frac{p}{2}}|} \quad (6)$$

The magnitude of α was estimated to be 0.77±0.02 in the range of 0.005 V s^{-1} to 0.225 V s^{-1}, suggesting a step-wise mechanistic pathway in the peak region of the voltammogram, where the reaction requires more energy to proceed and the change in reaction kinetics occurs [44,48].

3.3. Influence of temperature

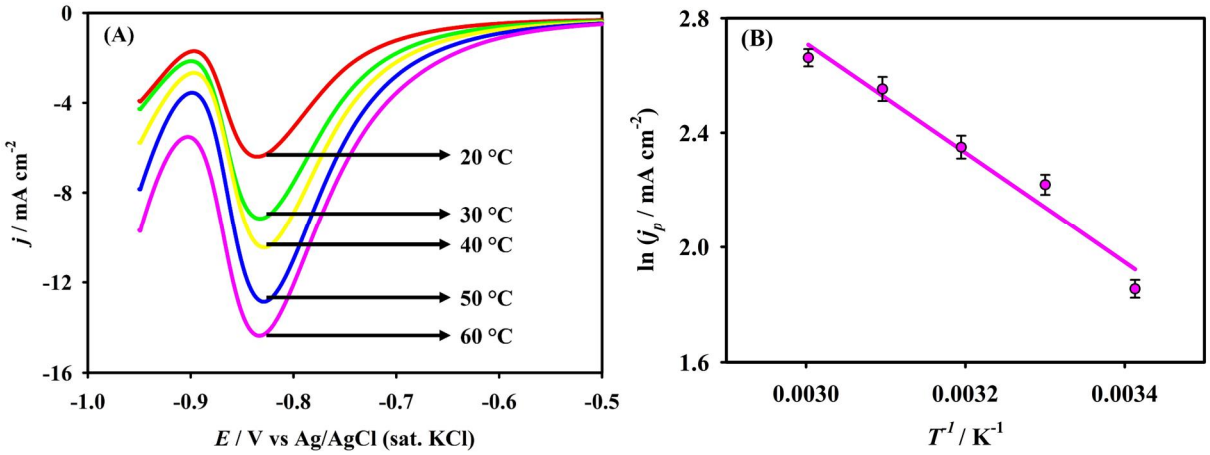

Figure 6. (A) Temperature dependent voltammograms of Pt electrode recorded in 2.0 M KCl + 1.0 M $NaNO_2$ solution at 0.005 V s^{-1} scan rate. (B) Arrhenius plot for nitrite reduction current at Pt electrode obtained from Fig. 7(A).

Finally, effect of temperature on nitrate reduction in KCl medium was investigated on Pt surface to evaluate the activation energy. For this purpose, change in current of nitrite reduction was monitored at ca. –0.816 V in the temperature range 20 - 60 °C for 1.0 M $NaNO_2$ in 2.0 M KCl. **Figure 6(A)** shows the dependency of CV regarding nitrite reduction reaction on Pt electrode against various temperature. As the temperature increased, the diffusion of nitrite ions increased thereby enhancing the NO_2^- ion reduction current. Note that in case of electrochemistry, current response represents the reaction rate. Hence, Arrhenius equation (7) [50,51]:, in terms of current density instead of conventional reaction rate, was employed to evaluate activation energy (i) of nitrite reduction reaction under the experimental condition.

$$ln\, J = ln\, A - \frac{E_a}{RT} \qquad (7)$$

Here, J is the current density at a specific temperature observed at a fixed potential (–0.816 V in this case), A is the pre-exponential factor, and other symbols have their own meanings. The linearized form of Arrhenius equation, that is, the logarithm of peak current was linearly decreased with the reciprocal of absolute temperature (293-333K) yielding a straight line (see **Fig. 6(B)**) with a good correlation coefficient (i.e., $r^2 = 0.95$). The slope of this plot yielded the activation energy (E_a) of nitrite reduction at Pt electrode. The estimated activation energy of nitrite reduction reaction on Pt was ca. 19.8 kJ mol^{-1} with pre-exponential factor of ca. 8.39 $\times 10^3$ mA cm^{-2}. The calculated

value is smaller than the nitrite reduction reaction on Rh and Rh deposited graphite electrodes, indicating the reaction is more feasible on Pt electrode [50,51].

4. Conclusion

The present report represents the study of electrochemical reduction of NO_2^- ions under aerated condition using polycrystalline Pt electrode. From a fundamental point of view, reducing NO_2^- ion to a specific product is difficult due to competitive chemical steps. Maintaining neutral pH, we found NO as the product on polycrystalline Pt surface from adsorptive stripping analysis. In solution phase, NH_3 was found from the studies of Nessler reagent test and gas chromatography. Thorough kinetic investigation revealed that NO_2^- ion receives an electron from Pt electrode surface and converts into NO, which in turn forms NH_3 on the electrode surface in reverse scan. Our next objective will be to construct a reactor to expand the current understanding of the nitrite reduction reaction because NH_3 is important in synthetic industrial applications.

Authors' contribution

Md. Fahamidul Islam: Writing-original draft, experimental and data analysis, **Hassan Shahriar Ifti:** Experimental and data analysis, Review and editing, **Mostafizur Rahman & Ali Aldalbahi:** Review and editing, and funding acquisition, **Kentaro Aoki:** Experimental and review, **Yuki Nagao:** Experimental and review, **Jamal Uddin:** Review and editing, **Mohammad A. Hasnat:** Conceptualization, writing-review & editing, supervision, and funding acquisition.

Acknowledgement

The authors acknowledge King Saud University, Riyadh, Saudi Arabia, for funding this work through Researchers Supporting Project number (RSP2024R30). In addition, the authors thank the Ministry of Education, Bangladesh (Grant No. PS20201512), Shahjalal University of Science and Technology Research Center (Grant No. PS/2023/1/02) and Noakhali Science and Technology University Research Center (Grant No. NSTU-RC-CHE-T-23-64) for partial supports.

Conflict of Interest

The authors declare that they have no known competing financial interests or personal relationships that could have appeared to influence the work reported in this paper.

References

1. Li, X., Ping, J., and Ying, Y. (2019) Recent developments in carbon nanomaterial-enabled electrochemical sensors for nitrite detection. *TrAC Trends Anal. Chem.*, **113**, 1–12.
2. Cockburn, A., Heppner, C.W., and Dorne, J.L.C.M. (2014) Environmental Contaminants: Nitrate and Nitrite. *Encycl. Food Saf.*, **2**, 332–336.
3. Ciji, A., and Akhtar, M.S. (2020) Nitrite implications and its management strategies in aquaculture: a review. *Rev. Aquac.*, **12** (2), 878–908.
4. Joint FAO/WHO Expert Committee on Food Additives. Meeting (44th : 1995 : Rome, I., and International Program on Chemical Safety. (1996) Toxicological evaluation of certain food additives and contaminants in food. 465.
5. Neth, M.R., Love, J.S., Horowitz, B.Z., Shertz, M.D., Sahni, R., and Daya, M.R. (2020) Fatal Sodium Nitrite Poisoning: Key Considerations for Prehospital Providers. *https://doi.org/10.1080/10903127.2020.1838009*, **25** (6), 844–850.
6. (1995) Environmental Medicine.
7. Gupta, S.K., Gupta, A.B., and Gupta, R. (2017) Pathophysiology of Nitrate Toxicity in Humans in View of the Changing Trends of the Global Nitrogen Cycle With Special Reference to India. *Indian Nitrogen Assess. Sources React. Nitrogen, Environ. Clim. Eff. Manag. Options, Policies*, 459–468.
8. Cockburn, A., Brambilla, G., Fernández-Cruz, M.L., Arcella, D., Bordajandi, L.R., Cottrill, B., van Peteghem, C., and Dorne, J. Lou (2013) Nitrite in feed: From Animal health to human health. *Toxicol. Appl. Pharmacol.*, **270** (3), 209–217.
9. Nagababu, E., Ramasamy, S., and Rifkind, J.M. (2006) S-Nitrosohemoglobin: A mechanism for its formation in conjunction with nitrite reduction by deoxyhemoglobin. *Nitric Oxide*, **15** (1), 20–29.
10. Maia, L.B., and Moura, J.J.G. (2014) How biology handles nitrite. *Chem. Rev.*, **114** (10), 5273–5357.
11. Choi, J., and Batchelor, B. (2008) Nitrate reduction by fluoride green rust modified with copper. *Chemosphere*, **70** (6), 1108–1116.
12. Gago, B., Lundberg, J.O., Barbosa, R.M., and Laranjinha, J. (2007) Red wine-dependent reduction of nitrite to nitric oxide in the stomach. *Free Radic. Biol. Med.*, **43** (9), 1233–1242.
13. Shwu-Ling, P., Chong, N.M., and Chen, C.H. (1999) Potential applications of aerobic denitrifying bacteria as bioagents in wastewater treatment. *Bioresour. Technol.*, **68** (2), 179–185.
14. Taguchi, S., and Feliu, J.M. (2007) Electrochemical reduction of nitrate on Pt(S)[n(1 1 1) × (1 1 1)] electrodes in perchloric acid solution. *Electrochim. Acta*, **52** (19), 6023–6033.
15. Hasnat, M.A., Islam, M.A., and Rashed, M.A. (2015) Influence of electrode assembly on catalytic activation and deactivation of a Pt film immobilized H+ conducting solid electrolyte in electrocatalytic reduction reactions. *RSC Adv.*, **5** (13), 9912–9919.
16. Hasnat, M.A., Ben Aoun, S., Nizam Uddin, S.M., Alam, M.M., Koay, P.P., Amertharaj, S., Rashed, M.A., Rahman, M.M., and Mohamed, N. (2014) Copper-immobilized platinum electrocatalyst for the effective reduction of nitrate in a low conductive medium: Mechanism, adsorption thermodynamics and stability. *Appl. Catal. A Gen.*, **478**, 259–266.

17. Duca, M., Van Der Klugt, B., Hasnat, M.A., MacHida, M., and Koper, M.T.M. (2010) Electrocatalytic reduction of nitrite on a polycrystalline rhodium electrode. *J. Catal.*, **275** (1), 61–69.
18. Mao, R., Zhu, H., Wang, K.F., and Zhao, X. (2021) Selective conversion of nitrate to nitrogen gas by enhanced electrochemical process assisted by reductive Fe(II)-Fe(III) hydroxides at cathode surface. *Appl. Catal. B Environ.*, **298**, 120552.
19. Zhang, R., Wang, S., Chou, S., and Jin, H. (2022) Research Development on Aqueous Ammonium-Ion Batteries. *Adv. Funct. Mater.*, **32** (25), 2112179.
20. Yüzbaşıoğlu, A.E., Avşar, C., and Gezerman, A.O. (2022) The current situation in the use of ammonia as a sustainable energy source and its industrial potential. *Curr. Res. Green Sustain. Chem.*, **5**, 100307.
21. Valera-Medina, A., Amer-Hatem, F., Azad, A.K., Dedoussi, I.C., De Joannon, M., Fernandes, R.X., Glarborg, P., Hashemi, H., He, X., Mashruk, S., McGowan, J., Mounaim-Rouselle, C., Ortiz-Prado, A., Ortiz-Valera, A., Rossetti, I., Shu, B., Yehia, M., Xiao, H., and Costa, M. (2021) Review on ammonia as a potential fuel: From synthesis to economics. *Energy and Fuels*, **35** (9), 6964–7029.
22. Djinović, P., and Schüth, F. (2015) Energy Carriers Made from Hydrogen. *Electrochem. Energy Storage Renew. Sources Grid Balanc.*, 183–199.
23. He, X., Hu, L., Xie, L., Li, Z., Chen, J., Li, X., Li, J., Zhang, L., Fang, X., Zheng, D., Sun, S., Zhang, J., Ali Alshehri, A., Luo, Y., Liu, Q., Wang, Y., and Sun, X. (2023) Ambient ammonia synthesis via nitrite electroreduction over NiS2 nanoparticles-decorated TiO2 nanoribbon array. *J. Colloid Interface Sci.*, **634**, 86–92.
24. Wang, H., Zhang, F., Jin, M., Zhao, D., Fan, X., Li, Z., Luo, Y., Zheng, D., Li, T., Wang, Y., Ying, B., Sun, S., Liu, Q., Liu, X., and Sun, X. (2023) V-doped TiO2 nanobelt array for high-efficiency electrocatalytic nitrite reduction to ammonia. *Mater. Today Phys.*, **30**, 100944.
25. Ouyang, L., He, X., Sun, S., Luo, Y., Zheng, D., Chen, J., Li, Y., Lin, Y., Liu, Q., Asiri, A.M., and Sun, X. (2022) Enhanced electrocatalytic nitrite reduction to ammonia over P-doped TiO2 nanobelt array. *J. Mater. Chem. A*, **10** (44), 23494–23498.
26. Cai, Z., Ma, C., Zhao, D., Fan, X., Li, R., Zhang, L., Li, J., He, X., Luo, Y., Zheng, D., Wang, Y., Ying, B., Sun, S., Xu, J., Lu, Q., and Sun, X. (2023) Ni doping enabled improvement in electrocatalytic nitrite-to-ammonia conversion over TiO2 nanoribbon. *Mater. Today Energy*, **31**, 101220.
27. Liang, J., Deng, B., Liu, Q., Wen, G., Liu, Q., Li, T., Luo, Y., Alshehri, A.A., Alzahrani, K.A., Ma, D., and Sun, X. (2021) High-efficiency electrochemical nitrite reduction to ammonium using a Cu3P nanowire array under ambient conditions. *Green Chem.*, **23** (15), 5487–5493.
28. Arikawa, Y., Otsubo, Y., Fujino, H., Horiuchi, S., Sakuda, E., and Umakoshi, K. (2018) Nitrite Reduction Cycle on a Dinuclear Ruthenium Complex Producing Ammonia. *J. Am. Chem. Soc.*, **140** (2), 842–847.
29. Sun, C., Li, F., An, H., Li, Z., Bond, A.M., and Zhang, J. (2018) Facile electrochemical co-deposition of metal (Cu, Pd, Pt, Rh) nanoparticles on reduced graphene oxide for electrocatalytic reduction of nitrate/nitrite. *Electrochim. Acta*, **269**, 733–741.
30. G. Casella, I., and Contursi, M. (2014) Highly dispersed rhodium particles on multi-walled carbon nanotubes for the electrochemical reduction of nitrate and nitrite ions in acid medium. *Electrochim. Acta*, **138**, 447–453.

31. Shin, H., Jung, S., Bae, S., Lee, W., and Kim, H. (2014) Nitrite reduction mechanism on a Pd surface. *Environ. Sci. Technol.*, **48** (21), 12768–12774.
32. Troutman, J.P., Li, H., Haddix, A.M., Kienzle, B.A., Henkelman, G., Humphrey, S.M., and Werth, C.J. (2020) PdAg Alloy Nanocatalysts: Toward Economically Viable Nitrite Reduction in Drinking Water. *ACS Catal.*, **10** (14), 7979–7989.
33. Li, H., Guo, S., Shin, K., Wong, M.S., and Henkelman, G. (2019) Design of a Pd-Au Nitrite Reduction Catalyst by Identifying and Optimizing Active Ensembles. *ACS Catal.*, **9** (9), 7957–7966.
34. Seraj, S., Kunal, P., Li, H., Henkelman, G., Humphrey, S.M., and Werth, C.J. (2017) PdAu Alloy Nanoparticle Catalysts: Effective Candidates for Nitrite Reduction in Water. *ACS Catal.*, **7** (5), 3268–3276.
35. Liu, Q., Wen, G., Zhao, D., Xie, L., Sun, S., Zhang, L., Luo, Y., Ali Alshehri, A., Hamdy, M.S., Kong, Q., and Sun, X. (2022) Nitrite reduction over Ag nanoarray electrocatalyst for ammonia synthesis. *J. Colloid Interface Sci.*, **623**, 513–519.
36. Gadde, R.R., and Bruckenstein, S. (1974) The electroduction of nitrite in 0.1 M HClO4 at platinum. *J. Electroanal. Chem. Interfacial Electrochem.*, **50** (2), 163–174.
37. Duca, M., Kavvadia, V., Rodriguez, P., Lai, S.C.S., Hoogenboom, T., and Koper, M.T.M. (2010) New insights into the mechanism of nitrite reduction on a platinum electrode. *J. Electroanal. Chem.*, **649** (1–2), 59–68.
38. Hasnat, M.A., Rashed, M.A., Alam, M.S., Rahman, M.M., Islam, M.A., Hossain, S., and Ahmed, N. (2010) Electrocatalytic reduction of NO2−: Platinum modified glassy carbon electrode. *Catal. Commun.*, **11** (13), 1085–1089.
39. Duca, M., Cucarella, M.O., Rodriguez, P., and Koper, M.T.M. (2010) Direct reduction of nitrite to N2 on a Pt(100) electrode in alkaline media. *J. Am. Chem. Soc.*, **132** (51), 18042–18044.
40. Duca, M., Van Der Klugt, B., and Koper, M.T.M. (2012) Electrocatalytic reduction of nitrite on transition and coinage metals. *Electrochim. Acta*, **68**, 32–43.
41. Chun, H.J., Apaja, V., Clayborne, A., Honkala, K., and Greeley, J. (2017) Atomistic Insights into Nitrogen-Cycle Electrochemistry: A Combined DFT and Kinetic Monte Carlo Analysis of NO Electrochemical Reduction on Pt(100). *ACS Catal.*, **7** (6), 3869–3882.
42. Cerrón-Calle, G.A., Fajardo, A.S., Sánchez-Sánchez, C.M., and Garcia-Segura, S. (2022) Highly reactive Cu-Pt bimetallic 3D-electrocatalyst for selective nitrate reduction to ammonia. *Appl. Catal. B Environ.*, **302**, 120844.
43. Winter, M.J. d-Block Chemistry Mark J. Winter.
44. Mumtarin, Z., Rahman, M.M., Marwani, H.M., and Hasnat, M.A. (2020) Electro-kinetics of conversion of NO3− into NO2− and sensing of nitrate ions via reduction reactions at copper immobilized platinum surface in the neutral medium. *Electrochim. Acta*, **346**, 135994.
45. Bard, A.J., and Faulkner, L.R. (2001) Basic Potential Step Methods. *Electrochem. Methods Fundam. Appl.*, 156–225.
46. Shabik, M.F., Hasan, M.M., Alamry, K.A., Rahman, M.M., Nagao, Y., and Hasnat, M.A. (2021) Electrocatalytic oxidation of ammonia in the neutral medium using Cu2O.CuO film immobilized on glassy carbon surface. *J. Electroanal. Chem.*, **897** (May), 115592.
47. Alam, M.S., Rahman, M.M., Marwani, H.M., and Hasnat, M.A. (2020) Insights of temperature dependent catalysis and kinetics of electro-oxidation of nitrite ions on a

glassy carbon electrode. *Electrochim. Acta*, **362**, 137102.
48. Islam, M.F., Islam, M.T., Hasan, M.M., Rahman, M.M., Nagao, Y., and Hasnat, M.A. (2022) Facile fabrication of GCE/Nafion/Ni composite, a robust platform to detect hydrogen peroxide in basic medium via oxidation reaction. *Talanta*, **240**, 123202.
49. González Velasco, J. (1997) Determination of standard rate constants for electrochemical irreversible processes from linear sweep voltammograms. *Electroanalysis*, **9** (11), 880–882.
50. Brylev, O., Sarrazin, M., Bélanger, D., and Roué, L. (2006) Rhodium deposits on pyrolytic graphite substrate: Physico-chemical properties and electrocatalytic activity towards nitrate reduction in neutral medium. *Appl. Catal. B Environ.*, **64** (3–4), 243–253.
51. Protsenko, V.S., and Danilov, F.I. (2011) Activation energy of electrochemical reaction measured at a constant value of electrode potential. *J. Electroanal. Chem.*, **651** (2), 105–110.